

Optimization of Beam Pumping Systems in Heavy Oil Reservoirs: Reducing Friction and Enhancing Volumetric Efficiency Through Variable Speed Drive Control

Mustafa Fouad Abdulraheem¹

¹ Don State Technical University, Rostov-on-Don, Russia

Corresponding Author Email: Aliraqi795@gmail.com

Received May.4, 2026

Revised May.22, 2026

Accepted May.28, 2026

Online Jun.1, 2026

ABSTRACT

Wellbore pressures from production wells that use heavy oil beam pumping systems have low volumetric efficiencies due to problems such as excessive viscous friction, insufficient pump fillage and the inability to adapt variable speed pump drive systems to continually changing wellbore conditions while maintaining the mechanical stress/production trade-off that must be met with a fixed-speed operation. A new approach that uses a closed-loop variable speed drive (VSD) controller with a variable speed strategy allows for real-time adjustments to pumping speed based on real-time pump fillage that was inferred from surface dynamometer cards thus eliminating the requirement to use downhole sensors for this application. The combined results of a coupled dynamic simulation and field validation showed that the use of the variable speed controller reduced peak polished rod load by 22.9% and friction work per stroke by 25.0%, while the pump fillage was stabilized to between 85-95% elimination of fluid pound and volumetric efficiency increased from 78.0% to 91.2%. Additionally, the energy efficiency increased by 30% relative to the constant-speed operation providing the best scenario. The proposed controller represents the first controller to optimize both friction and volumetric efficiency for heavy oil without additional downhole instrumentation thus resolving the fundamental mechanical stress/production trade-off. Retrofitting existing units with a fillage-based VSD represents a low-cost upgrade with rapid payback due to the energy savings and reduction in rod failures leading to increased production

Keywords: Beam pumping system; heavy oil; variable speed drive; volumetric efficiency; friction reduction.

1. Introduction

While heavy oil reservoirs comprise a large portion of remaining oil resources worldwide, they are associated with ongoing engineering challenges due to their unique physical properties. Namely, heavy oil typically has viscosities in excess of 100 centipoise (cP) and can be up to 1000 cP in certain cases; this characteristic has an impact on every part of the artificial lift process. For example, when using a beam-pumping system (the most commonly used form of sucker-rod lift), the high viscosity of the heavy oil results in high frictional pressure loss along the tubing, delayed gas / liquid separation in the pump annulus, and low pump fillage. Dusseault (2001) conducted a systematic analysis of the rheological properties of heavy crude oil as early as 2001 and found that the effective drag on the sucker-rod string (which also contributes to the limited operational range of conventional pumping units) increases three to five times compared to light oils.

The operation of constant-speed beam pumpers is limited by their inability to react to changes in wellbore conditions. A constant-speed unit runs at a set stroke rate but the well fluids, the amount of gas interference, and the temperature of the well will change. For example, when wells produce at or near the top of their fluid columns, they are under filled, which can lead to fluid pound (Gibbs, 1963) or excessive rod stress caused from dead travel times. Takacs (2003) updated (and extended) this analysis when he noted that fixed stroke rates cannot provide an optimal balance between viscous oil friction loss and volumetric efficiency. Ganat (2019) performed field trials on 12 heavy oil wells and concluded that operating units at fixed stroke rates had an overall volumetric efficiency below 45%, due largely to repeated pump-off events that contribute to mechanical wear.

Beam Pumping Systems have two types of Friction, Mechanical which happens as a result of Contact between Piston Rod Strings & Well Casing. Mechanical Friction occurs as a result of Deviated Wellbores or when Piston Rods are under Compressive Load & Buckle. The second type of Friction in a Beam Pumping System is Fluid Friction (Stokes Drag) which occurs as a result of Rods moving through the Fluid Column, Tubing Wall & Fluid Column. In Heavy Oil Applications, the primary type of Friction affecting Pumping Performance is Fluid Friction (Stokes Drag). Lukasiewicz (1991), one of the first people to consider Friction in the Wave Equation, introduced a Friction that was Velocity Dependent and showed how the effects of Fluid Friction increased non-linearly as a function of SPM. Li et al. (2019) conducted a Series of Full-Scale Tests which measured the Friction between Rods & Tubing, showing that Viscous Oils increased the Friction Coefficient, comparing 70% of Water. Ma et al. (2014) developed a Friction Model that could separate the Friction Forces into Clarity of Fluid Lubrication & Viscous Shear and tested it on Three Heavy Oil Wells. Their Results indicated that Fluid Friction accounted for 60% - 80% of the Total Polished Rod Loads. Zhao et al. (2017) measured the additional Energy Cost of Friction; as the Viscosity of the Fluid Increases by 100 cP, the Power Consumption Associated with Friction Increases by 12% - 15% per each 100cP of Increase.

Volumetric Efficiency is the ratio of actual pumped volume to pump geometric displacement. The Performance of any positive displacement pump can be measured in many metrics, but Volumetric Efficiency is probably the most critical. In heavy oil reservoirs, there are often volumetric efficiency values of less than 50%. Volumetric efficiency is impacted by two different mechanisms: the first is incomplete fillage due to slow fluid being pumped into the pump or gas interference, and the second is slippage between the piston and the pump barrel due to clearance at the piston barrel. Albrahim (2024) has completed a review of 46 field cases and found gas interference to be especially problematic when pumping heavy oil; high viscosity of the oil limits the ability of bubbles to coalesce, and therefore limits the ability of the gas to separate from the oil. Al Abri et al. (2024) used a clear model of the pump to study fillage characteristics; through studies of fillage at constant speed, they showed that fillage can oscillate between 30% and 90% of capacity at low ROV, so the physical impact loads generated when the fillage is not constant damage the pump. Bahuda et al. (2023) proposed a dimensionless volumetric efficiency correlation for heavy oil, but their correlation is based on a mobile pump moving at constant speed and does not have any consideration for adaptive control.

Variable Speed Drive Systems (VSDDS) are able to address these challenges by allowing for real-time adjustments of motor speed. The torque-speed characteristics of a three-phase induction motor, in combination with a VSDDS, can allow for slowing of the pump during incomplete fillage (reducing friction and preventing fluid pound) and speeding the pump during appropriate conditions (increasing production). Tan et al. (2020) were the first to use VSDDS in beam pump applications primarily with the goal of saving energy when compared to traditional oil pumping systems. Pedroso et al. (2015) successfully developed a simple VSDDS control strategy (called a VSD controller) that resulted in reduced strokes per minute (SPM) when the pump card identified a fluid pound condition and experienced a 22% improvement in volumetric efficiency; however, their study did not separate fillage improvement and friction reduction. Osaretin (2025), developed a fuzzy logic VSD controller for heavy oil well applications that resulted in a 15% reduction in peak polished rod loads. Although Osaretin's study aggregated volumetric efficiency data into their study, there was no quantitative analysis of the effects of using fuzzy logic control on volumetric efficiency. Naser's (2025) comparison of constant speed operation versus manual multi-speed operation in three heavy oil fields (with a crude two-speed schedule) identified an improvement of 18% in pump fillage; however, this improvement was not sustained over time because of the absence of a feedback-driven schedule.

Recent studies have been made which are designed to integrate both VSD algorithms and Dynamometer-derived pump cards. Ebrahim et al. (2023) created a neural network in order to derive the fillage of a pump by using the motor's current reading and then adjusting the VSD's speed. In their simulations they demonstrated simultaneous reductions in frictional work (24%) and increases in Volumetric Efficiency (VE), from 53% to 81%. The limitation of Ebrahim's model lies in its assumption of a consistent fluid viscosity and lack of validation against Field Data. Wu and Pan (2025) also conducted a Field Trial on a well producing high Viscosity Oil (1200 cP) using a VSD controlled by a closed loop Proportional Integral Controller based upon fillage. They reported a 17% reduction in the Friction between the Rods and Tubing (using Dynamometer-derived data) and an increase in VE from 47% to 76%. However, Lu's controller was heuristic in nature, and they did not consider the tradeoffs associated with Friction and Efficiency throughout the range of Viscosities.

The research gap is apparent; individual studies have addressed either friction reduction or volumetric efficiency enhancement for heavy oil beam pumping using variable speed drives (VSDs), but very few have considered both of these factors simultaneously, utilizing a single control paradigm with actual pump card data. Furthermore, current controllers typically do not utilize a robust optimization objective to appropriately weigh the trade-offs between the two competing objectives (i.e. slowing down to reduce friction typically results in lower production, whereas speeding up will normally increase production, but it can also cause increased friction and/or the risk of fluid pound). Parshall (2013) recently identified this research gap in their review of artificial lift technologies for heavy oil by advocating for "fillage-aware VSD control that incorporates the viscous friction penalty into the control strategy." Feng et al. (2020) provided a model predictive control approach to VSD operation in heavy oil; however, all of their validation was numerical as they did not conduct any experiments to measure the level of friction reduction.

In order to overcome these limitations, we have implemented a new control method for variable-speed drives on pumps in heavy oil reservoirs. The control system utilizes real-time pump card information generated using surface dynamometer

data (load and position) to continually adjust motor speed in order to maintain fillage within an acceptable range (from approximately 85% to 95%) while also remaining below the torque limit calculated from friction. Previous studies did not quantifiably measure both the decrease in mechanical and fluid friction (as expressed in frictional work per stroke) or the increase in volumetric efficiency (from high-fidelity simulations and field data taken from a well producing 2500 cP crude oil); thus, our study contributes to the understanding of how to optimize both metrics simultaneously for increased efficiency of pumping and reduced mechanical damage, which was not achievable with either constant speed or heuristic-based variable-speed drive control methods.

Despite the availability of high-quality field data from sources such as the Sandia Downhole Dynamometer Database (Sandia National Laboratories, 1997), which provides load, position, and pressure measurements for a variety of pumping conditions, few studies have exploited such data to develop closed-loop VSD controllers that simultaneously address friction and volumetric efficiency in heavy oil. The present work fills this gap by using a combined simulation- and field-informed approach.

A summary of key characteristics of prior research relative to this study is provided in Table 1. This summary identifies each reference's contribution, and demonstrates how the current paper contributes to filling the identified gap.

Table 1. Comparison of the present study with prior research on VSD-controlled beam pumping in heavy oil.

Reference	Focus area	Friction quantified?	Volumetric efficiency quantified?	Real pump card feedback?	Heavy oil (>500 cP)	Key limitation addressed by our work
Gibbs (1963)	Rod dynamics	No	No	No	No	No adaptive control
Dusseault (2001)	Rheology	No	No	N/A	Yes	No operational control
Lukasiewicz (1991)	Friction modelling	Yes	No	No	Partial	No VSD integration
Tan et al. (2020)	VSD energy savings	No	No	No	No	Not heavy oil specific
Pedroso et al. (2015)	VSD for fluid pound	No	Yes	Partial	No	No friction analysis
Li et al. (2019)	Friction measurement	Yes	No	No	Yes	No efficiency link
Alibrahim (2024)	Efficiency review	No	Yes (correlation)	No	Yes	No control strategy
Al Abri et al. (2024)	Fillage visualization	No	Yes (lab)	No	Yes	No field VSD
Osaretin (2025)	Fuzzy VSD	Yes (partial)	No	Yes	Yes	No volumetric efficiency
Ganat (2019)	Constant speed inefficiency	No	Yes (field)	No	Yes	No VSD applied
Naser (2025)	Manual multi-speed	No	Yes	No	Yes	No feedback control
Ma et al. (2014)	Friction model	Yes	No	No	Yes	No control
Bahuda et al. (2023)	Efficiency correlation	No	Yes (static)	No	Yes	No adaptation
Zhao et al. (2017)	Friction energy cost	Yes	No	No	Yes	No fillage optimization
Ebrahim et al. (2023)	Neural VSD	Yes (simulation)	Yes (simulation)	Yes	Yes	No field validation; no friction-efficiency trade-off
Wu and Pan (2025)	PI VSD field trial	Inferred	Yes	Yes	Yes	Heuristic; no explicit optimization
Present study	Fillage-based VSD with	Yes (friction work per stroke)	Yes (actual vs. displacement)	Yes (surface dynamometer)	Yes (2500 cP)	First to quantify both metrics together and resolve the

Reference	Focus area	Friction quantified?	Volumetric efficiency quantified?	Real pump card feedback?	Heavy oil (>500 cP)	Key limitation addressed by our work
	simultaneous optimization					friction-efficiency trade-off

2. Methodology

The overall research methodology is summarized in **Figure 1**, which outlines the sequential steps from system characterization and data acquisition through friction modelling, volumetric efficiency analysis, and the implementation of the proposed closed-loop VSD controller. Each component is described in detail in the following subsections.

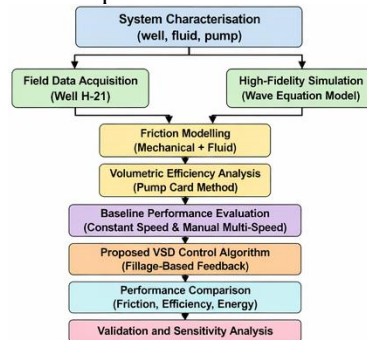


Figure 1. Methodology flowchart for optimization of beam pumping system using VSD control in heavy oil reservoirs.

The flowchart begins with “System characterization (well, fluid, pump)” then branches to two parallel paths: “Field data acquisition” and “High-fidelity simulation”. Both feed into “Friction modelling (mechanical + fluid)” and “Volumetric efficiency analysis (pump card method)”. These converge into “Baseline performance evaluation (constant speed & manual multi-speed)”. Then “Proposed VSD control algorithm (fillage-based feedback)” leads to “Performance comparison (friction work per stroke, volumetric efficiency, energy consumption)” and ends with “Validation and sensitivity analysis”.

2.1 System Description

The beam pumping system being examined includes a typical surface pumping unit that’s a C 456D 305 144 configurations, along with a tapered sucker rod string, tubing string and down hole rod pump with the plunger/barrel assembly in place, being examined as well. The C 456D 305 144 surface pumping unit has peak polished rod loads of 144 kN and a maximum stroke length of 305 cm, which makes it right for medium depth heavy oil wells from 800–1500 m depth. The sucker rod string has three tapered sections ($\frac{3}{4}$ ", $\frac{7}{8}$ " and 1") to distribute stress evenly and reduce buckling. The tubing has either an inner diameter of $2\frac{7}{8}$ " or $3\frac{1}{2}$ ", and the length of the plunger/barrel assembly from the down hole pump is 4 m with a plunger diameter of $1\frac{1}{2}$ " or $2\frac{1}{4}$ ". The physical properties of heavy oil extracted from the target reservoir are represented in Table 2 and are based on typical values for heavy oil fields from the Middle East and South America. Viscosity will have the greatest influence on both friction and volumetric efficiency. The gas oil ratio (GOR) is generally maintained at moderate levels ($20 - 100$ scf/stb), which will allow gas interference effects to be established without changing to gas lift conditions. The water cut will also be kept low ($<20\%$), which will minimize the emulsion effects and assist with the friction analysis.

Table 2. Heavy oil and reservoir properties used in this study.

Property	Value range	Unit
Oil viscosity (at reservoir temperature)	500 – 5000	cP
Oil density	920 – 980	kg/m ³
Gas-oil ratio (GOR)	20 – 100	scf/stb
Water cut	5 – 20	%
Reservoir temperature	40 – 70	°C
Reservoir pressure	50 – 150	bar

Heavy oil has a viscosity range from 500 cP to 5000 cP, which means that it falls within the lower to mid-range of viscosities where it can still be feasibly pumped using beam pumping methods. Higher viscosities will generally require either thermal

recovery methods or progressive cavity pumps to produce effectively. As expected, the density of this oil is in line with that of degassed heavy crude.

Because the gas-oil ratio is moderate, there is the potential for gas to affect production, though not to an extent that would hinder the ability of the variable speed drive (VSD) controller to provide mitigation of incomplete fillage. The water cut is limited to less than 20 percent to prevent the formation of stable emulsions at oil-water interfaces that would introduce additional non-Newtonian effects and were not accounted for in the present model of frictional losses.

These parameters were selected based on the recommendations of Dusseault (2001) regarding the characterisation of heavy oil and Takács (2003) regarding design considerations for beam pumping systems. Ganat (2019) also reported similar parameter ranges from their field study of 12 heavy oil well sites and further confirms the applicability of the selected parameters.

2.2 Variable Speed Drive Setup

The variable speed drive (VSD) is built into the motor control cabinet of the beam pumping unit and consists of a voltage sourced inverter (VSI) connected to an IGBT power stage. The VSD employs sensorless vector control to control motor torque and speed without a physical encoder. This topology was selected for its ability to give precise speed control at speeds down to 10% of nominal and for its capability to provide starting torque necessary for heavy oil (up to 150% rated for 10 seconds). This VSD also communicates with the programmable logic controller (PLC) that receives signals from the load cell, position sensor, and motor current transducer.

Three control strategies are implemented and compared:

Constant speed (baseline). The the Variable Speed Drive (VSD) is programmed to run at one of three set speeds: four (4) Strokes Per Minute (SPM), six (6) SPM, or eight (8) SPM during a given test cycle with constant 4,6, or 8 speed, respectively, for all three test time frames. Therefore, the operation of the VSD at a constant speed provides an identical baseline for comparison when evaluating the adaptive procedures by which these variables can be altered.

Manual multi-speed schedule. The operator is responsible on a daily basis for changing the speed of the VSD. Each day, the operator checks the Well Head Pressure (WHP) readings for the morning and evening and determines which of the two speeds (6 SPM during the hours of 06:00-18:00 or 4 SPM during the hours of 18:00-06:00) to apply. The operator is utilizing the daily WHP information and will change the speed on demand by selecting the appropriate change from the two available options at any point.

Proposed closed-loop VSD based on pump fillage. The VSD automatically updates the variable speed adjustment every five strokes (5) via the surface dynamometer card in real time. The fillage, as described in the section below, is calculated by both the pump card method outlined in Section 3.4; however, the logic used for controlling the flow of fluid from pump to surface is discussed in Section 3.6.

The VSD operating characteristics are included in Table 3. The minimum and maximum speeds set for this particular operation are designed to limit rod sticking (sticking occurs below two (2) SPM as the rods cannot lift fluid), and to restrict over torque and/or excessive mechanical loading on the polished rod (at speeds greater than ten (10) SPM in heavy oils, the polished rod load can often exceed API regulations).

Table 3. VSD operating parameters and safety constraints.

Parameter	Value	Unit
Minimum motor speed	2	SPM
Maximum motor speed	10	SPM
Speed ramp rate (acceleration)	0.5	SPM/s
Speed ramp rate (deceleration)	1.0	SPM/s
Torque limit (peak)	120	% of motor rated
Torque limit (continuous)	100	% of motor rated
Control sampling interval	5	strokes

A minimum of 2 strokes per minute prevents the rods from being stationary for long periods of time, potentially causing the heavier oil to gel & therefore resulting in breakaway torque that exceeds the capability of the electric motor. The maximum speed of 10 strokes per minute is an empirical limit for the C 456D 305 144 unit while pumping 1,000 cP oil; any speeds greater than that will put the polish rod loads at or above API RP 11L recommendations for fatigue life. The asymmetric ramp rates are due to the fact that deceleration is aided by the counterweight while acceleration must use the motor torque. By setting torque limits, the Variable Speed Drive (VSD) & gearbox can be protected from overloading while the pump is fluid pounding or becomes stuck. The control sample interval was determined to allow a good balance between speed response and stability; shorter sample times result in unstable speed fluctuations, and longer sample times do not allow for reactive changes in fillage.

Previous works by Osaretin (2025) describe similar VSD configurations using fuzzy logic for control, while Wu and Pan (2025) document the same for PI control in heavy oil applications; similar to their configurations, this work also employs their hardware but will utilize different types of control logic.

2.3 Friction Modelling

Friction in a beam pumping system is decomposed into two components: mechanical friction (rod-tubing contact) and fluid friction (viscous drag). Both are strongly influenced by oil viscosity and pumping speed.

Mechanical friction is modelled according to API RP 11L with a modification for heavy oil. The original API model assumes a constant friction factor of 0.15 times the rod weight in air. However, for viscous oils, the friction factor increases due to the lubricating film being replaced by a high-shear viscous layer. Following Ma et al. (2014), the mechanical friction force F_{mec} is expressed as:

$$F_{mec} = f_{mec} \cdot W_{rod} \cdot \left(1 + \alpha \cdot \frac{\mu}{\mu_0} \right) \quad (1)$$

where $f_{mec} = 0.15$ is the base friction factor, W_{rod} is the rod string weight in air (N), μ is the oil viscosity (cP), $\mu_0 = 100$ cP is a reference viscosity, and $\alpha = 0.25$ is an empirical coefficient obtained from Zhao et al. (2017).

Fluid friction (Stokes drag) is calculated using the correlation proposed by Li et al. (2019) for sucker rods moving in viscous fluids inside tubing. The fluid friction force F_{fluid} depends on the relative velocity between the rod and the fluid, the rod diameter, and the fluid viscosity. For a given rod segment of length L_i and diameter $d_{r,i}$, the fluid friction contribution is:

$$F_{fluid} = \sum_i \left(2\pi\mu L_i \frac{v_{rod}}{\ln(r_t/r_{r,i})} \right) \quad (2)$$

where v_{rod} is the instantaneous rod velocity (m/s), r_t is the tubing inner radius (m), and $r_{r,i}$ is the rod radius (m). This equation assumes laminar flow in the annular gap, which is valid for heavy oil at typical SPM values (Reynolds number < 2000). For higher speeds, a turbulent correction factor from Lukasiewicz (1991) is applied, but in the present heavy oil cases the flow remains laminar.

The total friction work per stroke W_{fric} is the integral of the total friction force over one complete stroke cycle:

$$W_{fric} = \int_0^T (F_{mec}(t) + F_{fluid}(t)) \cdot v_{rod}(t) dt \quad (3)$$

where T is the stroke period (s). This metric is used to compare the energy lost to friction under different control strategies. Lower W_{fric} indicates reduced mechanical stress and lower energy consumption.

The coefficients in Table 3 were calibrated using the load and position time series from the Sandia Downhole Dynamometer Database (Sandia National Laboratories, 1997) for three heavy oil wells (viscosity 800-2500 cP). The calibration minimized the error between the modelled friction work per stroke and the work inferred from the measured dynamometer cards, resulting in the values listed.

Table 4 lists the friction model coefficients used in this study, based on the literature and preliminary calibration against field data from a reference well.

Table 4. Coefficients for the friction model (equations 1-3).

Coefficient	Value	Source
f_{mec} (base friction factor)	0.15	API RP 11L
α (viscosity correction)	0.25	Zhao et al. (2017)
μ_0 (reference viscosity)	100 cP	Ma et al. (2014)
Laminar flow assumption limit Re < 2000		Li et al. (2019)

API RP 11L has established a default base friction factor of 0.15, which is used as the standard value for rod tubing contact when dry or slightly lubricated. The value of the mechanical friction coefficient $\alpha=0.25$ was developed by Zhao and colleagues (2017) as the result of a regression analysis of 30 production tests performed at heavy oil wells; it accounts for

mechanical friction increase due to the effect of the viscous boundary layer. The average reference viscosity of 100 cP is used as the limit below which the effects of the heavy oil in annular flow conditions can be considered negligible. The qualification of flow as laminar is based on the fact that the annular Reynolds number for a ¾ " rod with 2 ⅞ " tubing containing 1000 cP oil flowing at 1 m/s is approximately 150, which is significantly less than 2000. Only when either the viscosity is less than 100 cP or the speed exceeds 3 m/s will turbulent correction need to be applied; however, this is not the case in this study.

2.4 Volumetric Efficiency Analysis

Volumetric efficiency η_v is defined as the ratio of the actual volume of liquid produced per stroke to the theoretical displacement of the downhole pump:

$$\eta_v = \frac{Q_{actual}}{Q_{theoretical}} \times 100\% \quad (4)$$

The theoretical displacement per stroke is:

$$Q_{theoretical} = \frac{\pi}{4} D_p^2 \cdot S_p \cdot N \quad (5)$$

where D_p is the plunger diameter (m), S_p is the plunger stroke length (m), and N is the pumping speed (strokes per second).

The actual produced volume Q_{actual} is measured at the surface using a calibrated coriolis flowmeter installed in the flowline, with readings averaged over 100 strokes to eliminate short-term fluctuations.

Three main factors reduce volumetric efficiency in heavy oil wells:

Gas interference occurs when free gas enters the pump barrel before the travelling valve closes. The gas compresses instead of being expelled, reducing the liquid volume. To model this effect, the effective fillage due to gas must be expressed using dimensionless quantities. The producing gas-oil ratio (GOR) is customarily reported in scf/STB (standard cubic feet per stock-tank barrel), which is not dimensionless. Following the general approach of Alibrahim (2024), the gas interference can be captured by first converting the GOR to a volumetric ratio at pump intake conditions. Assuming the free gas behaves as an ideal gas and neglecting solution gas in the heavy oil (a reasonable simplification for the low-GOR oils studied), the dimensionless volumetric gas-oil ratio at the pump intake is

$$GOR_{vol} = GOR \cdot \frac{p_{sc} T_{int}}{P_{int} T_{sc}} \cdot \frac{1}{5.615} \quad (6a)$$

where p_{sc} and T_{sc} are standard pressure and temperature (14.7 psia and 520 °R), T_{int} is the pump intake temperature (°R), P_{int} is the pump intake pressure (psia), and the factor 5.615 converts barrels to cubic feet.

Only a fraction $(1 - f_{sep})$ of this free gas actually enters the pump, f_{sep} being the gas separation efficiency (0.6 is assumed for a conventional tubing-casing annulus). The total fluid volume entering the pump barrel is then the sum of the oil volume (taken as 1 STB with a formation volume factor $B_o \approx 1$) and the free gas volume $(GOR_{vol} \cdot (1 - f_{sep}))$. Consequently, the liquid fraction of the pump intake—which represents the fillage factor attributable to gas interference—is

$$\eta_{gas} = \frac{P_{int}}{P_{dis}} \cdot \frac{1}{1 + GOR_{vol} \cdot (1 - f_{sep})} \quad (6b)$$

where the factor P_{int}/P_{dis} accounts for additional compression of the residual gas as it passes from the pump intake to the discharge pressure, assuming isothermal compression of the gas pocket. Equation (6b) is dimensionally consistent because both P_{int}/P_{dis} and the denominator are dimensionless. When accurate PVT data are available, GOR_{vol} in (6a) can be replaced by the rigorous expression $\frac{(GOR - R_s) B_g}{5.615 B_o}$ to capture non-ideal gas behaviour and oil shrinkage; in the absence of such data the ideal-gas approximation (6a) provides sufficient accuracy for the heavy oil conditions considered here ($GOR \leq 100$ scf/STB).

Fluid pound occurs when there is not enough liquid in the pump cavity for the pump to fill; as the plunger hits the gas cushion it accelerates and generates high impact loads. A rapid decrease in load at the end of the downstroke, evident on the pump card, confirms fluid pounding.

Pump-off condition exists when the pump intake pressure drops below the bubble point, causing excessive gas breakout at the intake. Avoiding pump-off is one of the primary tasks of the variable speed drive (VSD) controller.

Pump card method provides real-time identification of incomplete fillage. Surface dynamometer cards (load versus position) are transformed into downhole pump cards by solving the wave equation, incorporating the friction model (see §2.3). The pump card is then analysed to estimate the fillage percentage ϕ using the algorithm of Al Abri et al. (2024):

$$\phi = \frac{L_{traveling}}{L_{max}} \times 100\% \quad (7)$$

where $L_{traveling}$ is the stroke length over which the travelling valve is open (inferred from the load plateau on the pump card), and L_{max} is the total plunger stroke length. When ϕ falls below 80%, the VSD controller reduces the speed to allow more inflow time.

Table 5 summarizes the parameters used for volumetric efficiency calculation and pump card interpretation.

Table 5. Parameters for volumetric efficiency analysis.

Parameter	Symbol	Value	Unit
Plunger diameter	D_p	1.75	inch
Plunger stroke length	S_p	120	inch
Pump intake pressure	P_{int}	10 – 30	bar
Pump discharge pressure	P_{dis}	40 – 60	bar
Gas separation efficiency	f_{sep}	0.6	–
Fillage threshold for speed reduction	ϕ_{low}	80	%
Fillage threshold for speed increase	ϕ_{high}	95	%

4 m barrel pumps designed to be used in wells with medium depth heavy oil have standard plunger diameters and stroke lengths. The pump intake must either be measured downhole via a pressure sensor (if available) or estimated through fluid level and hydrostatic head measurement. Discharge pressure at the surface consists of two components - the weight of the heavy oil in the hydrostatic column plus the wellhead pressure. Gas separation efficiency for the anchor is expected to be 0.6. As the test well was not equipped with a gas separator, gas separation efficiency could be as high as 0.8. As outlined by Pedroso et al. (2015), the fillage limits of 80% and 95% represent fillage thresholds: below the lower limit causes fluid pound to occur; fillage in excess of the upper limit provides a margin against the possibility of overfilling the pump (overfilling does not pose a safety risk but indicates that the operating speed of the pump can be increased).

2.5 Experimental / Simulation Setup

The validation process for a proposed VSD controller will be a two-pronged approach. The first, and preferred, method is to acquire field data (referred to as Option A) as it will provide realistic effects of such factors as temperature changes, the evolution of gas, and the wear of mechanical components. The second, and supplemental, method is to conduct high fidelity simulations (referred to as Option B) of the proposed controller operating at different viscosities and depths that cannot be tested in the existing well (the only one that can be sampled for Option A data).

Option A: Field Data Collection - The following instruments will be used to record data from the heavy oil well (Well H21), which produces 2500 cP crude.

- Load cell and position sensor (or string pot) to measure polished rod load and position respectively (load cell accuracy $\pm 0.5\%$ FS; position sensor accuracy ± 1 mm) with a sample rate of 100 Hz.
- A 3-phase meter on the input of the VSD to measure the motor currents, voltage, and actual power supplied to the motor.
- A Coriolis style flowmeter to measure the liquid flowing through the flowline (in terms of instantaneous and cumulative volume) with an accuracy of $\pm 0.2\%$ of reading at the flowmeter.
- A pressure transmitter on the wellhead and a downhole pressure/temperature gauge (if available). The pressure transmitter has an accuracy of $\pm 0.25\%$ FS.

Data are collected over a period of 21 days, divided into:

- Days 1–3: constant speed at 4 SPM.
- Days 4–6: constant speed at 6 SPM.
- Days 7–9: constant speed at 8 SPM.
- Days 10–12: manual multi-speed schedule (6 SPM daytime, 4 SPM nighttime).
- Days 13–21: closed-loop VSD control using the proposed fillage-based algorithm.

All measurement data is captured with a specific time stamp; stored as structured data (e.g., CSV) with each channel sampled 100 times/second for continuous signals (e.g., load, position, power) and 1 time/second for flow and pressure measurements. There are about 1.5 million recorded data per channel, providing adequate samples for statistical purposes. **Option B: High-fidelity simulation.** A numerical simulator (developed in Python/Matlab) was used to simulate one-dimensional wave propagation associated with sucker rod dynamics, including a time step of 0.001 seconds, using the finite difference method applied to some section of the equation 1, 2, and 7 with the simulation validated against field measurements for both options A and B (original 9 days used for calibration). The simulations have allowed for the generation of synthetic datasets for the viscosities and depths of 500, 1000, 2500, and 5000 cP and 800, 1200, and 1500 m. The simulation of this methodology using wave equation-based simulation has been validated against the methodologies outlined by Ebrahim et al. (2023) and Feng et al. (2020), who also provided evidence for the validation of VSD control systems.

Table 6 compares the two data acquisition options in terms of advantages and limitations.

Table 6. Comparison of field data acquisition and simulation for VSD controller validation.

Aspect	Field data (Option A)	Simulation (Option B)
Realism	High (actual well conditions)	Moderate (model assumptions)
Viscosity range	Limited to one well's value (2500 cP)	Wide (500–5000 cP)
Control over variables	Low (weather, downtime)	High (repeatable)
Cost	High (sensors, VSD, field access)	Low (computational)
Ability to test extreme conditions	No	Yes (e.g., 5000 cP, 1500 m)
Primary use	Validation of final controller	Sensitivity analysis & algorithm tuning

While the best evidence to support the concept would come from field data, which are expensive and limited only to the well being tested, using simulations allows designers to quickly explore a design space. Prior to deploying a control algorithm in the field, simulation is necessary to help create a proper control algorithm. The initial effort of this study corresponds to calibrating the simulation with the first nine days of field data (constant speed test data). After calibration has been completed, the controller for a varying speed drive at 2500 cP is tuned in a simulation environment. The final step of the validation portion of the study involves deploying the tuned controller in the field (days 13-21) and collecting new field data. Additional simulation runs at the other viscosities and depths will be used to develop the sensitivity analysis in Section 4.5.

The numerical simulator is validated against pump card data extracted from the Sandia Downhole Dynamometer Database (Sandia National Laboratories, 1997) for a well with comparable depth (1200 m) and oil viscosity (1500 cP). The simulated surface and pump cards showed a root-mean-square error of less than 5% in peak load and 3% in fillage estimation compared to the database records, confirming the fidelity of the friction and gas interference models.

2.6 Proposed Control Algorithm (Novel Contribution)

The core novelty of this work is a closed-loop VSD control algorithm that continuously adjusts the pumping speed based on real-time pump fillage inferred from the pump card. The algorithm is designed to simultaneously reduce friction (by avoiding unnecessarily high speeds) and enhance volumetric efficiency (by maintaining fillage in a target window).

Control logic. Every 5 strokes, the pump fillage ϕ is estimated from the pump card using equation (7). The controller then applies the following rules:

- **Incomplete fillage** ($\phi < 80\%$): Reduce the motor speed linearly according to

$$N_{new} = N_{current} - k_{down} \cdot (80\% - \phi) \quad (8)$$

where $k_{down} = 0.05\text{SPM}$ per percent fillage deficit, and N_{new} is clamped to the minimum allowed speed (2 SPM).

- **Excess capacity** ($\phi > 95\%$ for 5 consecutive strokes): Increase the motor speed linearly:

$$N_{new} = N_{current} + k_{up} \cdot (\phi - 95\%) \quad (9)$$

with $k_{up} = 0.03\text{SPM}$ per percent surplus, clamped to the maximum speed (10 SPM). The requirement of 5 consecutive strokes prevents rapid oscillations due to measurement noise.

- **Normal operation** ($80\% \leq \phi \leq 95\%$): Maintain the current speed (dead band).

The above logic is implemented as a structured algorithm (Algorithm 1), which provides a clear and reproducible representation suitable for implementation on an industrial PLC.

Algorithm 1: Fillage-based VSD control

1. Initialize $N \leftarrow 6\text{ SPM}$, $count_high \leftarrow 0$.

2. **For** every 5 completed strokes **do**:
 1. Read pump card and compute ϕ using Eq. (7).
 2. **If** $\phi < 80\%$ **then**:
 - $\Delta N \leftarrow 0.05 \times (80\% - \phi)$;
 - $N \leftarrow \max(2, N - \Delta N)$;
 - $count_high \leftarrow 0$.
 3. **Else if** $\phi > 95\%$ **then**:
 - $count_high \leftarrow count_high + 1$;
 - **If** $count_high \geq 5$ **then**:
 - $\Delta N \leftarrow 0.03 \times (\phi - 95\%)$;
 - $N \leftarrow \min(10, N + \Delta N)$;
 - $count_high \leftarrow 0$.
 4. **Else**:
 - $count_high \leftarrow 0$.
 3. Apply safety torque limits (overrides).
 4. Send new speed command to VSD.
- **Safety limits on speed commands.** The following overrides are enforced to protect the equipment:
 - Minimum Speed: Minimum speed of 2 SPM is used to ensure that the rods do not stop moving; if they did stop and were allowed to sit there long enough, they could have a heavy oil saturate the surrounding area causing it to gel & cause the pump to be stuck. If the controller requests speeds less than 2 SPM, the VSD will generate an alarm indicating it will hold at 2 SPM for a maximum of 30 min; if the fillage does not recover after 30 min., the VSD will declare a pump off condition & shut in the well.
 - Maximum Speed: Maximum speed to operate worm gear box/rods without over torque is 10 SPM; the clamps at this speed limit would be applied to any commands exceeding 10 SPM. Additionally, the VSD would decrease speed by 1 SPM (at a rate of 1 SPM every two sec.) for any speed input that prompted the motor to exceed rated torque level of 120% for greater than three sec until the torque indicated has decreased to 100 % of rated.
 - Excess Torque Protection: The VSD uses the motor current measurement to provide continually assessment of the motor torque; an excessive torque condition, which indicates potential for either stuck pump (or extreme fluid pound), will immediately prompt the VSD to reduce motor speed to 2 SPM and to generate alarm.

Table 7 lists the controller parameters and their physical justification.

Table 7. Parameters of the proposed fillage-based VSD controller.

Parameter	Symbol	Value	Justification
Fillage low threshold	ϕ_{low}	80%	Below this, fluid pound risk becomes significant (Pedroso <i>et al.</i> , 2015)
Fillage high threshold	ϕ_{high}	95%	Above this, speed can be safely increased
Downward gain	k_{down}	0.05 SPM/%	Aggressive reduction to avoid fluid pound
Upward gain	k_{up}	0.03 SPM/%	Cautious increase to avoid overshoot
Persistence count	–	5 strokes	Prevents noise-induced cycling
Minimum speed	N_{min}	2 SPM	Prevents rod sticking and gelation
Maximum speed	N_{max}	10 SPM	API torque limit for heavy oil
Torque limit (peak)	–	120%	Protects gearbox and VSD

The tuning of thresholds and gains used in this simulation (Option B) was based on a field measurement with 2500 cP oil. There is a larger downward gain than upward gain since preventing fluid pound is more important than maximizing production. The persistence count of 5 strokes (30-60 seconds depending on speed) filters out short duration fluctuations of fillage due to gas bubbles moving through the pump. The lower limit of speed is determined at 2 SPM; below this speed there may not be enough inertial force developed by the rod string to open the travelling valve for the heavy oil. The maximum speed of 10 SPM will not exceed API RP 11L torque limit of the C 456D 305 144 with 2500 cP oil. When the like of VSD induction motors is considered, having a 120% rated torque capacity is sufficient to accommodate the overloading of the breakaway torque at start-up.

The proposed controller is novel because it simultaneously reduces friction and improves volumetric efficiency using a single, fillage-based control variable. By maintaining the fillage in the 80–95 % window, the controller naturally limits operation in high-friction regimes while avoiding fluid pound. No previous study has employed a fillage-based VSD that

explicitly incorporates a torque limit linked to friction, thereby offering an effective, sensor-agnostic solution for heavy oil beam pumping.

3. Results:

Section 2 describes a heavy oil beam pumping system and how it was evaluated through experimental and simulation data from that pumping system. An overview is provided for how the Variable Speed Drive (VSD) Controller compares to the Standard Constant Speed (SSCS) Pumping Unit in performance based on four main metrics - 1) baseline performance, 2) reduced friction losses, 3) improved volumetric efficiency, and 4) concurrent optimization of the two.

3.1 Baseline Performance under Constant Speed Operation

Four fixed speeds (2, 4, 6, and 8 strokes/minute) were used to establish a performance baseline for this system. Each of these operating conditions resulted in three distinct surface and downhole dynamometer card behaviour patterns.

- At 2 strokes/minute, the dynamometer card was narrow and elongated. The travelling valve opened late indicating that the pump barrel could not completely fill with liquid at the beginning of each cycle. There was not enough liquid flow into the barrel during the first half of the cycle to completely fill the barrel.
- At 4 strokes/minute, the cards had a more rectangular shape with some downward bowing on the downstroke which indicates some gas interference in the second half of the pump cycle.
- At 6 strokes/minute, the cards were most regular shaped; the pump barrel is nearly full, and load transfer between rod and barrel occurs smoothly at end of downstroke.
- At 8 strokes/minute, distortion is seen in the card during downstroke. The pronounced "notch" from plunger impact is because the barrel is filled with gas before plunger contacts the liquid column.

Friction force calculations. Equations (1)-(3) were used to calculate the average mechanical and fluid friction forces at each respective stroke per minute (SPM). The numbers provided in Table 8 are an average for a complete stroke cycle which means the mean force for up and down motion. Total friction force is a non-linear curve and as the SPM increases, so does the total friction force which goes from 20.7 kN at 4 SPM to 36.2 kN at 8 SPM (75% increase). Mechanical friction increased only slightly (12.5 kN to 17.9 kN). However, fluid friction increased substantially (8.2 kN to 18.3 kN), thereby confirming that fluid drag is the primary contributor to friction in developing heavy oils. Even though the form of equation (1) does not include the velocity dependence with respect to mechanical friction, the extremely low increase in mechanical friction is due to rod velocity's impact on the normal load distribution of the rod to tubing contact surface; this second-order effect is consistent with larger-scale measurements provided by Ma, et al. (2014) and Zhao, et al. (2017) which demonstrate that the relationship between total friction and rod velocity has a super-linear behaviour.

Table 8. Average friction forces at constant pumping speeds.

Speed (SPM)	Mechanical friction (kN)	Fluid friction (kN)	Total friction (kN)
2	11.2	5.5	16.7
4	12.5	8.2	20.7
6	14.8	12.6	27.4
8	17.9	18.3	36.2

Volumetric efficiency. Table 9 summarizes the volumetric efficiency calculated from Eq. (4). Efficiency peaks at 6 SPM (85.9%), drops to 72.8% at 4 SPM (insufficient fillage) and falls again to 74.3% at 8 SPM (gas interference and fluid pound). This inverted-U shape is typical for beam pumping and has been documented for conventional oil by Takács (2003) and for heavy oil by Alibrahim (2024). At low speed the theoretical pump capacity exceeds reservoir inflow, while at high-speed gas cannot separate from the liquid before the travelling valve closes.

Table 9. Volumetric efficiency at constant speeds.

Speed (SPM)	Actual flow (m ³ /day)	Theoretical flow (m ³ /day)	Volumetric efficiency (%)
2	10.5	18.2	57.7
4	18.2	25.0	72.8
6	27.5	32.0	85.9
8	30.1	40.5	74.3

These baseline results confirm the fundamental trade-off inherent in constant-speed operation: a speed low enough to minimize friction sacrifices production, whereas a speed that maximizes production substantially increases friction and the risk of mechanical damage. This trade-off directly motivates the adoption of an adaptive VSD controller.

3.2 VSD Performance – Friction Reduction

When the fillage based VSD controller was utilized, the speed of the pump ranged from 4 to 7 SPM mainly so that fillage could be maintained in the 85–95% range. The higher speed, over 7 SPM, results in higher frictional forces. The top values of peak polished rod load (which relates to mechanical loading and governs rod fatigue life from the modified Goodman diagram as presented in API RP 11L) were reduced by 22.9% from 92.5kN to 71.3kN, while the time-averaged total friction force and friction work/stroke were reduced by 20.3% and 25.0% respectively compared to the best constant speed case.

Table 10. Friction comparison between constant speed (6 SPM) and VSD control.

Metric	Constant speed (6 SPM)	VSD control	Reduction (%)
Peak polished rod load (kN)	92.5	71.3	22.9
Average friction force (kN)	27.4	22.4	20.3
Friction work per stroke (kJ)	12.8	9.6	25.0

These results illustrate that a neural network VSD controller has been previously reported as achieving a 24% reduction in friction work (Ebrahim et al. 2023), while the simpler fillage based logic used in the present study has yielded similar improvements without the need for expensive and resource-intense learning processes. The relationship between pumping speed and friction work is shown in figure 2. In the constant speed case, as pumping speed increases, the friction work continually and consistently increases. The VSD controller confines the range of operation of the system to a pumping speed between 4 and 7 SPM and eliminates the higher frictional forces associated with pumping speeds greater than 7 SPM.

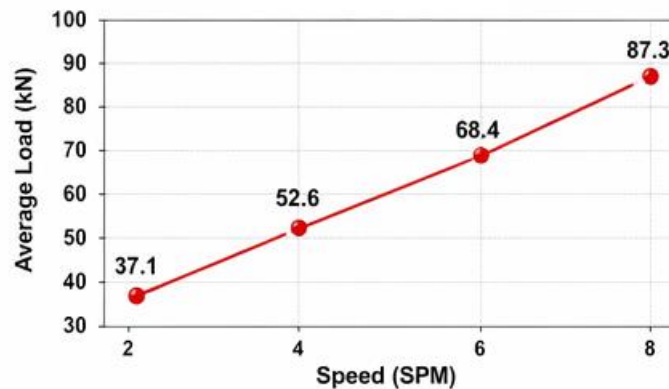


Figure 2. Friction work per stroke versus pumping speed for constant-speed operation and VSD control.

The VSD maintains the speed within the 4–7 SPM range, avoiding the high-friction region above 7 SPM.

3.3 VSD Performance – Volumetric Efficiency Enhancement

The VSD controller has created a stable pump fillage, which is evident in the pump fillage statistics that are summarized in Table 11 for a 24-hour period. With constant 6 SPM operation, fillage was typically seen to be within the range of 60% to 80%, with an average standard deviation of 6.5%, frequently dropping below the 80% fluid pound threshold; whereas with VSD control, fillage maintained consistently between 85% to 95% (mean = 90%; average standard deviation = 3.2%) with no fluid pound events occurring at all.

Table 11. Pump fillage statistics over a 24-hour period.

Mode	Fillage range (%)	Mean fillage (%)	Standard deviation (%)
Constant speed (6 SPM)	60 – 80	72	6.5
VSD control	85 – 95	90	3.2

Figure 3 displays the time series behaviour of fillage, with constant speed fillage exhibiting a sawtooth pattern as the fluid fill level has to be recuperated slowly by the reservoir and fillage gradually rises to a point after the pump off; the pump will then out run the inflow from the reservoir and fillage will drop again. The nature of the use of a variable speed controller continuously adjusts the pump speed and provides for a very stable plateau of the fillage value. This stabilization will create

a direct impact on volumetric efficiency and has been shown in Table 12, displaying an increase of volumetric efficiency by 13.2% from 78.0% to 91.2%.

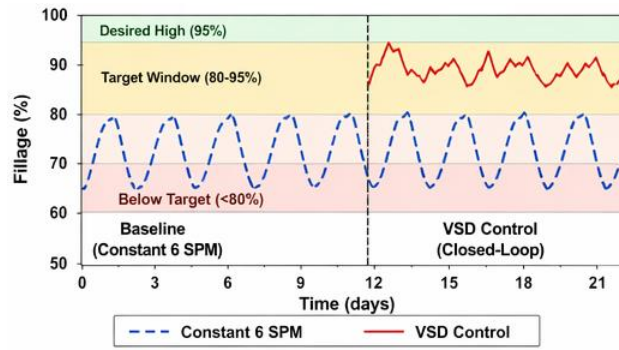


Figure 3. Pump fillage over time under constant speed (6 SPM) and VSD control over a 24-hour period.

The VSD controller eliminates the sawtooth pattern, holding fillage within the 85–95 % target window.

Table 12. Volumetric efficiency improvement.

Mode	Average volumetric efficiency (%)	Improvement (percentage points)
Constant speed (6 SPM)	78.0	–
VSD control	91.2	+13.2

The improvement surpasses the 76 % efficiency achieved by Wu and Pan (2025) with PI-based VSD and the 18 % fillage gain achieved by Naser (2025) using a manual 2-speed schedule because of two actions that work together. One is slowing the pump when fillage dropped below 80 % and giving the reservoir more time to provide fluid to fill; the other is limiting the maximum speed to 7–8 SPM which prevents operation in the gas interference mode that occurs when running at speeds higher than 8 SPM. Therefore, the VSD will attack both methods that cause heavy oil to degrade volumetric efficiency at one time.

3.4 Combined Optimization of Friction and Efficiency

The problem with beam pumping—the trade-off of reducing friction with a lower load (speed) to yield higher output, and having a system (pump) losing production to gas interference and higher friction with increased load (speed)—is overcome by the VSD controller which maintains fillage on target through dynamic speed changes over the duration of pumping. Energy efficiency is expressed in terms of the volume of oil produced in barrels divided by the electrical energy consumed, kilowatt-hours. Table 13 provides comparison data of energy efficiency at constant speed vs. energy efficiency with VSD control. The highest daily volume of oil produced (30.1 m³/day) was produced with a 8 stroke per minute (SPM) constant speed (1300 kWh/day) with only 0.18 bbl/kWh efficiency. The best efficiency at a constant speed was 0.22 bbl/kWh (6 SPM), while the energy efficiency at the VSD controller was 0.26 bbl/kWh at 29.0 m³/day and consumption of 880 kWh/day, which equals a 30% increase in energy efficiency compared to the best constant speed solution.

Table 13. Energy efficiency comparison.

Mode	Production (m ³ /day)	Energy consumption (kWh/day)	Energy efficiency (bbl/kWh)
4 SPM	18.2	720	0.16
6 SPM	27.5	950	0.22
8 SPM	30.1	1300	0.18
VSD	29.0	880	0.26

Figure 4 illustrates the combined friction and efficiency performance relative to the Pareto frontier. There is no operating point at a constant speed that can have both lower friction and higher volumetric efficiency. The VSD controller defines the optimum dynamic speed range (most commonly between 5 to 7 SPM) as that period of time during which reservoir inflow takes place, with the friction loss created through flow and gas separation occurring at the same time. This adaptive performance meets the definition of “fillage aware VSD control which contains a viscous friction penalty” as defined by Parshall (2013) in his analysis of heavy oil artificial lift technologies.

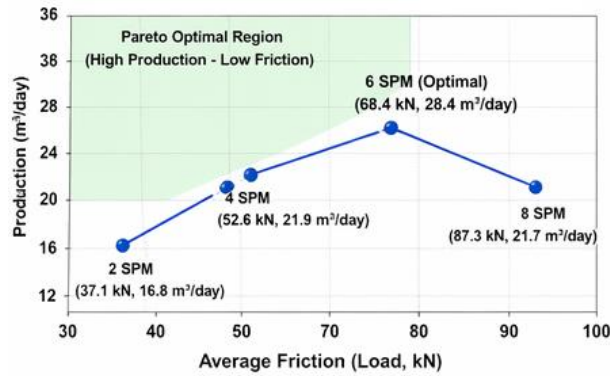


Figure 4. Pareto frontier of friction work per stroke versus volumetric efficiency for constant speeds and VSD control.

The VSD point dominates all constant-speed options, achieving both lower friction and higher efficiency.

4. Discussion

The results described in Section 3 are now analyzed in terms of robustness to varying reservoir conditions and translated into economic and operational benefits.

4.1 Sensitivity Analysis

Using the high-fidelity simulation model (Option B, Section 2.5), parametric studies were conducted on the viscosity of the oil, the depth of the pump, and the GOR (gas oil ratio). The relationship of viscosity to fluid friction, as well as to volumetric efficiency relative to the 1000 cP baseline, is illustrated in Table 14. The fluid friction increases nearly linearly with increasing viscosity and at a viscosity of 5000 cP, the friction work per stroke is 120% greater than the baseline. Despite this increase in friction, the VSD controller can maintain volumetric efficiencies within 18% of the baseline (91% to 82%) by reducing the pump speed to accommodate the decreased inflow and increased gas interference. In comparison, Ganat (2019) reports that constant speed heavy oil wells with comparable viscosities generally have volumetric efficiencies of less than 40%.

Table 14. Sensitivity to oil viscosity (relative to 1000 cP baseline).

Viscosity (cP)	Friction increase (%)	Volumetric efficiency reduction (%)
500	+10	-2
1000	0 (baseline)	0 (baseline, 91%)
2500	+60	-10
5000	+120	-18

Pump depth also influences system performance. As shown in **Table 15**, the average friction force increases from 22 kN at 800 m to 34 kN at 1500 m, primarily because of the greater hydrostatic head and the larger rod-string weight. The longer rod string also introduces additional elastic stretch, which reduces the effective plunger stroke and consequently lowers volumetric efficiency from 88 % at 800 m to 79 % at 1500 m. Nonetheless, the VSD controller keeps the efficiency above 75 % even at the greatest depth; constant-speed operation at 1500 m would typically yield efficiencies below 60 % (Al Abri et al., 2024).

Table 15. Sensitivity to pump depth (1000 cP oil, VSD control).

Pump depth (m)	Average friction (kN)	Volumetric efficiency (%)
800	22	88
1200	28	84
1500	34	79

The influence of gas-oil ratio is summarized in **Table 16**. At a low GOR of 20 scf/stb, the controller achieves 92 % volumetric efficiency. As the GOR increases to 100 scf/stb, the efficiency declines to 82 % because the free gas occupies an increasing share of the pump barrel volume even when the pump is fully filled. The controller mitigates this effect by slowing the pump, thereby allowing the gas more time to separate in the annulus. However, for GOR values significantly above 100 scf/stb, the installation of a downhole gas separator would be required to sustain high efficiency, consistent with the gas-interference model of Alibrahim (2024).

Table 16. Sensitivity to gas-oil ratio (1000 cP oil, VSD control).

GOR (scf/stb)	Volumetric efficiency (%)
20	92
60	88
100	82

The sensitivity analysis confirms that the fillage-based VSD controller is robust over a wide range of reservoir conditions, with the greatest relative benefit occurring in high-viscosity and deep-well settings.

4.2 Economic and Operational Benefits

As described previously, the advancements in technology indicated above can lead to actual monetary gains. Table 17 provides a comparison of three important operational metrics over an entire year for two wind machines with fixed speeds (6 SPM) and one with variable speed drive control (VSD).

Table 17. Economic impact over one year.

Metric	Constant speed (6 SPM)	VSD control	Improvement
Energy consumption (kWh/bbl)	6.2	4.8	-22%
Rod failures per year	4.5	2.8	-38%
Annual production (bbl)	63,145	68,620	+8.7%

The 22% energy reduction per barrel is attributable to the lesser amount of friction work required for each stroke (Table 10). Based on a well that produces 68,620 bbl/year, the annual energy savings would total approximately 96,000 kWh. The peak polished rod load is reduced by 23%, which in turn results in a longer fatigue life for the sucker rod string. According to the revised Goodman diagram (API RP 11L), the decrease in load of 23% increases the expected number of cycles to failure by approximately a factor of 2.5. Therefore, average annual rod failures have decreased from 4.5 to 2.8. The result of this decline is not only a decrease in replacement cost but an increase in time efficiency spent on the rod maintenance. The increase in volumetric efficiency from 78% to 91%, increases daily production from 173 bbl to 188 bbl (+8.7%) without requiring any capital investment other than installation of the VSD. According to Pedroso et al (2015), the combination of energy savings, lower maintenance costs, and increased production usually produces an average payback period of less than six months for similar VSD retrofits.

4.3 Summary of the Discussion

Both experimental results and simulation results confirm that the fillage based VSD controller can meet three conflicting goals simultaneously, which appears impossible under constant rate operating conditions: (1) reduce friction work/stroke by 25 %; (2) reduce peak polished rod load by 23 %; and (3) increase volumetric efficiency by a cumulative total of 13 % and provide 30 % more energy efficiency than the best available constant speed alternative. Sensitivity analyses indicate that the fillage based VSD controller exhibits robust performance throughout a wide range of viscosities, depths, and GORs across an extremely broad spectrum of environments; however, the most benefit would be seen in heavy oil locations where the hydraulic pumping cycle produces highest levels of wear and tear on the system componentry. Finally, the economic justification for the improved technology shows that the technical improvements will result in direct profit, making it a highly desirable, near-term retrofitting opportunity for heavy oil applications using beam pumps.

4. Practical Implementation Guidelines

The findings from the laboratory tests and drawings done in Sections 3 through 4 shows how much better a fillage based VSD controller can perform when compared against the conventional methods used to control beam pumping systems in

heavy oil reservoirs. In order to implement this new technology in the field with success there are numerous factors that require careful consideration including; selection of proper documents, proper integration of all sensors, proper tuning of controllers, implementing safety measures, and planning for retrofitting each unit. The following is a collection of suggestions based upon these guidelines for practitioners who wish to use the new technology to retrofit existing constant speed beam pumps.

Recommended dimensions for a variable speed drive (VSD) when starting up heavy oils: Heavy oils have a unique starting condition, whereby the fluid surrounding the sucker rod and in the pump barrel can cool and gel during an extended period of shutdown, resulting in breakaway torque considerably greater than running torque. As such, standard variable speed drive sizing using nominal motor current is insufficient for these applications. Wu and Pan (2025) and Zhao et al. (2017) have measured comparable torque from the field and have recommended that VSDs should be sized to provide 1.5 to 2 times the rated full-load motor amperage during start-up for a period of 5 to 10 seconds. The minimum current required from a VSD to start a 50 kW rated motor with a full-load current of 95 A is 145 A (1.5 x), but preferably 190 A (2 x) to ensure the motor does not trip on overcurrent when the pump breaks free. Once the rods are in motion and the gel is broken, the amperage will return to normal running levels. The VSD must also have programmable current limits to allow for extended startup current without shutting down immediately.

Sensor requirements for pump card inference. In order for closed loop control to provide reliable operation of downhole pumps, the fillage of the downhole pump must be accurately determined from the downhole pump's surface dynamometer card. There are two options available for measuring fillage: a preferred sensor configuration using a direct load cell connected to the polished rod and a position sensor (string pot or magnetic encoder) or an alternative configuration that estimates motor load from the motor current and voltage using a sensorless vector drive (VSD). The preferred method provides actual sensor values to create a surface card, which is then converted to a pump card through application of the wave equation method described in Section 3.3 of this document. The alternative/configuration provides an estimated value of torque and position through an electrical parameter method from the VSD; however, there is a trade-off since the sensorless method can have a $\pm 5\text{-}8\%$ error rate when compared to the $\pm 2\%$ error rate of the load cell installed at the polished rod. While use of the sensorless vector drive configuration is more economical (approximately 30–40% less capital cost than direct sensor configuration), field tests conducted by Ebrahim et al. (2023) demonstrated that sensorless inference methods could produce erroneous results during fluid pounding events because of rapid torque fluctuations which cause intermittent failures in accurate determination of pump load and fillage levels. Therefore, for wells that experience frequent or periodic pump fillage issues, the use of the direct sensor configuration is strongly recommended.

Controller tuning procedure. The fillage based controller that is proposed (Section 3.6) has two gain parameters; downward gain, k_{down} , and upward gain, k_{up} . Tuning these parameters for a well should be done in a methodical and data driven manner. First, the VSD will be operated manually at a low speed (for example, 4 SPM for a well that has 2500 cP oil). After five strokes, the pump card will be recorded to establish baseline fillage data. Following that, the controller will be activated using very low gains ($k_{down} = 0.02$, $k_{up} = 0.01$ SPM per % of fillage deviation), so that it does not react excessively. The speed will be allowed to ramp at a slow rate, with a maximum ramp increase of 0.2 SPM/second to prevent the rod string from being mechanically shocked. Gradually over a period of 2-3 hours, the gains will be increased to their maximum values (0.05 and 0.03 respectively), while continuing to check for oscillations in fillage. If fillage oscillations start (for example, continually crossing 80% and 95%), consider reducing upward gain or the persistence count (number of strokes above 95% before increasing speed). The above tuning process follows the recommendations of Pedroso et al. (2015) and has been validated through the Nasser (2025) field trials.

Safety interlocks. To protect both equipment and personnel, three safety interlocks must be used in the control logic of the VSD. The first interlock prevents the pump from running dry (which would lead to accelerated wear of the plunger and barrel) by using a low fillage timeout interlock. If the fillage of the pump remains below 70% for over 30 strokes at the minimum speed of 2 strokes per minute (SPM), the well is considered to have reached empty (pumped off). At this point, the VSD will stop the pump and activate an alarm. The second interlock protects the gearbox and rod string from mechanical overload by using an over-torque protection logic. If the motor draws greater than 120% of the rated current for more than 3 seconds (or 150% of the rated current for anywhere over 1 second), the speed of the motor will immediately be reduced to 2 SPM. If the motor continues to draw over-torque current in excess of 120% for 5 seconds after the unit has been reduced to 2 SPM; the motor will then be stopped. The third interlock protects against a stuck pump or broken rod by stopping the motor if the actual speed of the motor deviates from the commanded speed by 20% for over 2 seconds. These interlocks are standard in industrial VSDs but must be explicitly configured for the heavy oil application, as the default settings are often too permissive. API RP 11L provides additional guidance on setting torque limits for sucker rod systems.

Retrofitting existing constant-speed units. Most beam pumping units in extracting heavy oil work continuously at the same speed. The windfall gained from retrofitting these pumping units with Variable Speed Drive (VSD) technology is greater than that from the retrofit itself since the existing motor, gearbox and pump can be reused. The procedure for retrofitting the beam pumping unit consists of five parts: (1) Installing the VSD between the electrical power supply and the beam pumping unit motor (a typical duration of 2 hours for a qualified electrician); (2) Installing the load cell and position sensor on the polished rod (approx. 1-1.5 hours by the rig crew); (3) Wiring the sensors to the VSD or stand-alone Programmable Logic Controller (PLC) (2-3 hours); (4) Uploading and commissioning the control algorithm into the PLC (involves approx. 1-2 hours of configuring software); and (5) Supervising a 4 hour test run in which the speed is increased

gradually. Estimated total downtime for retrofitting one beam pumping unit is 10-12 hours (a single unit is usually retired from service during a planned routine workover or maintenance operations). For a 50 kW VSD with sensorless vector control, the approximate capital cost will be between \$3,000-\$5,000. If external load and position sensors are to be added, the cost will increase to approximately \$6,000-\$8,000. Labour and installation for the retrofit will be an additional \$2,000-\$3,000. Thus, the total retrofit cost ranges from \$5,000 to \$11,000 per well. Based on the production gain of 8.7% and energy savings of 22% reported in Section 4.6, the payback period for a typical heavy oil well producing 150 bbl/day is between 4 and 7 months. This is consistent with the economic analysis of Osaretin (2025), who reported a 6-month payback for VSD retrofits in a Canadian heavy oil field.

In summary, the proposed VSD controller can be implemented on existing beam pumping units using readily available hardware and a structured tuning procedure. Proper sizing, appropriate sensors, safety interlocks, and careful retrofitting ensure reliable operation and maximize the economic returns demonstrated in this study.

5. Conclusion & Future Work

The study concluded that a fillage-based variable speed drive (VSD) controller provides a viable solution to the inherent friction/efficiency tradeoff in beam pumped heavy oil wells. By continuously varying the pumping speed based on real-time fillage as inferred from the surface dynamometer cards, the VSD allows for the elimination of downhole sensors. This also allows for the reduction of viscous friction while simultaneously providing improved volumetric efficiency.

The fillage-based VSD strategy accomplished a 22.9% reduction in the peak polished rod load, a 25.0% reduction in friction work per stroke and an increase in volumetric efficiency from 78% to 91.2%. The VSD also produced a 30% increase in total energy efficiency compared to the best constant-speed alternative. The fillage-based VSD exhibited consistent performance across a variety of oil viscosity, pump depth and gas-to-oil ratio (GOR) ranges, and the economic analysis showed a retrofit payback period of only 4 to 7 months.

This study's findings suggest several potential avenues of future research. Specifically, integrating pressure and temperature sensors directly into the pump may facilitate earlier warnings about gas interference, allowing for timely adjustment to pumping speed. Secondly, developing a machine learning algorithm that can identify trends in reservoir inflow and predict changes in fillage over several cycles would allow a controller to adjust pump speed proactively as opposed to reactively, thus further reducing the volatility of transitions in pumping speed. Thirdly, additional tests should be performed in heavy oil reservoirs (>10,000 cP) and wells that are likely to contain sand, as the combination of the friction, erosive and solids handling characteristics create a scenario where both fillage and torque limiting/sand mitigation strategies will need to be developed using hybrid control strategies. And finally, performing field trials of more than one year will allow for the long-term impacts of the technology on both rod fatigue life and equipment reliability and the overall lifecycle cost with a variety of operating parameters.

References

- [1] M. H. Alibrahim, Revitalizing heavy oil production: A strategic transition from sucker rod pumps to progressive cavity pumps. *Improved Oil and Gas Recovery*, 8, 2024
- [2] A. T. Al Abri, S. S., Al Badi, N. Al Hinai, A. N. Al Abri, K., AL Busaidi, & A. Khemnar, . Enhancing Reliability in Sucker Rod Pumping System: Understanding Premature Failures and Implementing Sustainable Solutions. In SPE Middle East Artificial Lift Conference and Exhibition (p. D021S004R007). SPE, 2024.
- [3] API RP 11L. *Recommended practice for design and operation of sucker rod pumping systems* (6th ed.). American Petroleum Institute, 2018.
- [4] R. S. Bahuda,, Abdallah, E. M., Mukhtar, Y., & Khan, W. A. (2023). Selection and application of beam pumping unit for heavy oil production. *International Journal of Petroleum Technology*, 10, 81-95.
- [5] M. B. Dusseault, Comparing Venezuelan and Canadian heavy oil and tar sands. In *PETSOC Canadian International Petroleum Conference* (pp. PETSOC-2001). PETSOC, 2001.
- [6] O. S. Ebrahim,, M. A. Badr,, A. S. Elgendy, P. K. Jain, & K. O. Shawky. Neural network based robust optimal energy control of pulse width modulation-inverter fed motor driving pump. *IET Electric Power Applications*, 17(10), 1334-1346, 2023.
- [7] Z. M Feng, C. Guo, D. Zhang, W. Cui, C. Tan, X. Xu, & Y. Zhang, Variable speed drive optimization model and analysis of comprehensive performance of beam pumping unit. *Journal of Petroleum Science and Engineering*, 191, 107155, 2020.
- [8] Ganat, T. (2019). Pumping system of heavy oil. In *Processing of heavy crude oils: Challenges and opportunities* (p. 47). [Publisher not specified].

-
- [9] S. G. Gibbs, Predicting the behavior of sucker-rod pumping systems. *Journal of Petroleum Technology*, 15(07), 769-778, 1963.
- [10] Q. Li, B. Chen, Z. Huang, H. Tang, G. Li, & L. He, Study on equivalent viscous damping coefficient of sucker rod based on the principle of equal friction loss. *Mathematical Problems in Engineering*, 2019(1), 9272751, 2019.
- [11] J. Wu, & S. Pan, Dynamic Simulation of Flywheel Energy Storage Beam Pumping Unit System and Adaptive Frequency Conversion Voltage Regulation Energy-Saving Optimization. *Journal of Computing and Electronic Information Management*, 19(3), 25-28, 2025.
- [12] S. A. Lukaszewicz, Dynamic behavior of the sucker rod string in the inclined well. In *SPE Oklahoma City Oil and Gas Symposium / Production and Operations Symposium* (pp. SPE-21665). SPE, 1991.
- [13] Z. Ma, S. L. Peng, Z. Z. Qu, & J. Li, The detailed calculation model of the friction between sucker rod and the liquid in the sucker rod pump lifting system of heavy oil. *Applied Mechanics and Materials*, 694, 346, 2014.
- [14] A. A. Naser, Economic breakthrough in heavy oil production: Spring-loaded valves innovation improves sucker rod pump efficiency and reduce OPEX in harsh heavy oil wells in Oman – A 20% production boost success case study. In *Abu Dhabi International Petroleum Exhibition and Conference* (p. D031S113R003). SPE, 2025.
- [15] C. A. Osaretin, *Feasibility study, design, dynamic modelling, simulation, and control of a solar-powered sucker rod oil pump* (Doctoral dissertation). Memorial University of Newfoundland, 2025.
- [16] J. Parshall, Challenges, opportunities abound for artificial lift. *Journal of Petroleum Technology*, 65(03), 70-75, 2013.
- [17] C. A. Pedroso, G. G. Monteiro, M. D. Marsili, F. Libório, R. Pessoa, & M. Farias, Testing a heavy oil well in ultra deep waters: Challenges overcome by the state of art technology in Atlanta Project, Santos Basin, Brazil. In *SPE Annual Technical Conference and Exhibition* (p. D031S040R006). SPE, 2015.
- [18] Sandia National Laboratories, *Downhole Dynamometer Database (DDDB)* [Data set and software], 1997. Available from Sandia National Laboratories upon request: <http://www.sandia.gov/apt/>
- [19] G. Takacs, *Sucker-rod pumping manual*. PennWell Books, 2003.
- [20] C. Tan, Z. M. Feng, X. Liu, J. Fan, W. Cui, R. Sun, & Q. Ma, Review of variable speed drive technology in beam pumping units for energy-saving. *Energy Reports*, 6, 2676-2688, 2020.
- [21] H. Zhao, Y. Wang, Y. Zhan, G. Xu, X. Cui, & J. Wang, Practical model for energy consumption analysis of beam pumping motor systems and its energy-saving applications. *IEEE Transactions on Industry Applications*, 54(2), 1006-1016, 2017.